Vol 10 No 2, February 2001
1009-1963/2001/10(02)/0139-06
Chinese Physics
© 2001 Chin. Phys. Soc.
and IOP Publishing Ltd

EXPERIMENTAL EVIDENCE OF THE SELF-SIMILARITY AND LONG-RANGE CORRELATIONS OF THE EDGE FLUCTUATIONS IN HT-6M TOKAMAK*

Wang Wen-hao(王文浩)[a], Yu Chang-xuan(俞昌旋)[a], Wen Yi-zhi(闻一之)[a], Xu Yu-hong(许宇鸿)[b], Ling Bi-li(凌必利)[b], Gong Xian-zu(龚先祖)[b], Liu Bao-hua(刘保华)[b], and Wan Bao-nian(万宝年)[b]

[a] *Department of Modern Physics, University of Science and Technology of China, Hefei* 230027, *China*

[b] *Institute of Plasma Physics, Chinese Academy of Sciences, Hefei* 230031, *China*

(Received 3 August 2000; revised manuscript received 12 September 2000)

For a better understanding of long timescale transport dynamics, the rescaled range analysis techniques, the autocorrelation function (ACF) and the probability distribution function (PDF) are used to investigate long-range dependences in edge plasma fluctuations in an HT-6M tokamak. The results reveal the self-similar characters of the electrostatic fluctuations with self-similarity parameters (Hurst exponent) ranging from 0.64 to 0.79, taking into consideration the $\vec{E}_{\rm r} \times \vec{B}$ rotation-sheared effect. Fluctuation ACFs of both the ion saturation current and the floating potential, as well as PDF of the turbulence-induced particle flux, have two distinct timescales. One corresponds to the decorrelation timescale of local fluctuations (μs) and the other lasts to the order of the confinement time (ms). All these experimental results suggest that some of the mechanisms of the underlying turbulence are consistent with plasma transport as characterized by self-organized criticality (SOC).

Keywords: self-similarity, long-range correlation, SOC
PACC: 5255, 5225, 5240

I. INTRODUCTION

It has been known that the anomalous transport in magnetically confined plasmas has a characteristic quality called self-similarity, i.e., transport by avalanches (relaxation through transport events of all sizes), which is independent of the underlying local fluctuation mechanisms.[1−3] This self-similarity concept is generally linked to the long-time correlations in the dynamics of the fluctuations. In order to delve deeper into this mechanism, a model based on the concept of the self-organized criticality (SOC) has been proposed.[4,5] According to the SOC model, the dominant scales in the transport dynamics without sheared flow are the system scales (the order of the confinement time) rather than the underlying local fluctuation scales; the addition of sheared flow into the dynamics leads to a reduction of the system-scale transport events. Comparative analyses of the edge plasma fluctuations based on experimental data in the absence of sheared flow from several devices have been made.[6−9] However, these measurements are done near the location of $\boldsymbol{E}_{\rm r}$=0 to avoid the influence of the plasma $\boldsymbol{E}_{\rm r} \times B$ rotation, where $\boldsymbol{E}_{\rm r}$ is the radial electric field and B the toroidal magnetic field. Thus, more detailed investigation of the turbulence-induced transport behaviour with sheared flow effect in the edge region is needed for testing the SOC models.

In this paper, we apply three statistical analysis techniques to the electrostatic fluctuations and the turbulence-induced particle transport flux measured by Langmuir probes in the edge region where $\boldsymbol{E}_{\rm r} \neq 0$ (having poloidal sheared flow velocity) on the HT-6M tokamak. The self-similarity of a time series fluctuation is usually reflected by its autocorrelation function (ACF) with a narrow peak around the time lag zero and a slowly decaying tail for long time lags. However, because of short available data sets, it is hard to accurately determine the long tail of an ACF in magnetic fusion devices. The rescaled range statistics (R/S) technique, proposed by Mandelbrot and Wallis[10] and based on a previous hydrological analysis by Hurst,[11] can be applied to determine this long-time dependence by way of evaluating the Hurst exponent (H). The effect of the sheared flow can be clearly described as the reduction in the value of the

*Project supported by the National Natural Science Foundation of China (Grant Nos. 19675036 and 19635020).

Hurst exponent. In addition, statistically, the self-similarity can also be characterized by the asymmetry of the probability distribution function (PDF) of the turbulence-induced particle flux.

The remainder of this paper is organized as follows. In sec.Ⅱ, the experimental set-up for the measurement of fluctuations and turbulence transport flux is described. An ACF plot of the ion saturation current fluctuations is also given here. The R/S analysis is technique employed to determine the self-similarity parameter is shown in sec. Ⅲ. Section IV is dedicated to the property of the local particle flux PDF. Finally, the conclusions are presented in section V.

Ⅱ. DESCRIPTION OF EXPERIMENTS

The experiments were conducted for the ohmically heated hydrogen discharges on the HT-6M tokamak with a major radius R=65 cm, minor radius a=18.5 cm defined by a full poloidal limiter, toroidal magnetic field B ≈0.9 T, plasma current $I_{\rm p}$ ≈65 kA, chord-averaged electron density $\overline{n} \approx 0.85 \times 10{\rm m}^{-3}$, and loop voltage $V_{\rm l} \approx$ 3V. Fig.1 plots some typical discharge waveforms (shot number 19509) of the discharge parameters above. We can see from Fig.1(a) that the plasma current lasts about 70 ms with a flat top of 20 ms (20–40 ms). In this current plateau, the parameters such as edge H_α emission and the vertical displacement $\Delta_{\rm t}$ of the plasma column do not obviously change (shown in Fig.1(b)). $\Delta_{\rm t}$ varies within 1 mm, which is less than the radial extension of the diagnostic probes (=2 mm, described as follows).

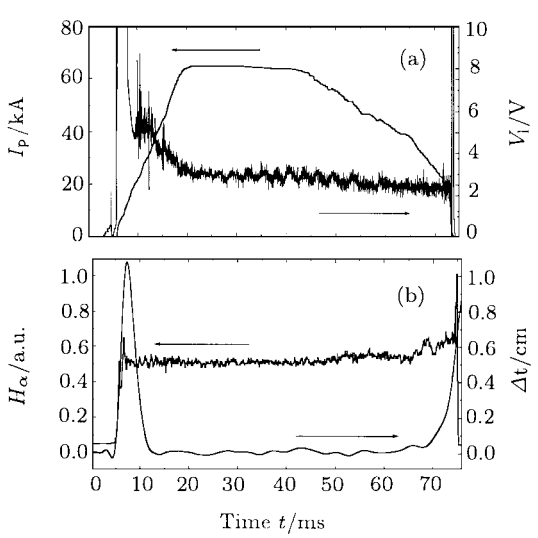


Fig.1. (a) Waveforms of plasma current $I_{\rm p}$ and loop voltage $V_{\rm l}$. (b) Edge H_α emission and the vertical displacement $\Delta_{\rm t}$ of the plasma column (shot number 19509).

The experimental set-up consists of two sets of probes mounted on the top of the tokamak along the central line, ∼ 180° toroidally displaced from the poloidal limiter. One square array of four identical tips (each tip 2 mm in length and 0.5 mm in diameter with 2 mm separation between adjacent tips, made of molybdenum wire), operated as a triple probe, was used to provide simultaneous and local measurements of equilibrium quantities of the ion saturation current $I_{\rm si}(t)$, electron temperature $T_{\rm e}(t)$, and density $n_{\rm e}(t)$, fluctuations of the ion saturation current $\tilde{I}_{\rm si}(t)$ and electron density $\tilde{n}_{\rm e}(t)$. Here $\tilde{I}_{\rm si}(t)$ (and the same as $\tilde{\phi}_{\rm f}(t)$ below) is directly obtained by isolating the direct part of a signal. The fluctuation $\tilde{n}_{\rm e}(t)$ can be estimated by $\tilde{n}_{\rm e}(t) = n_{\rm e}(t)\tilde{I}_{\rm si}(t)/I_{\rm si}(t)$ by neglecting $\tilde{T}_{\rm e}$.[12] Another array with one tip (tip 4) separated radially by 2 mm from other tips (other design parameters are the same as the former) was operated as four single Langmuir probes to simultaneously measure the equilibrium and fluctuating values of the floating potentials $(\phi_{\rm f}(t), \tilde{\phi}_{\rm f}(t))$, from which the equilibrium values of the radial electric fields $E_{\rm r}(t)$ and fluctuations of the poloidal electric fields $\tilde{E}_\theta(t)$ are deduced respectively (i.e., $E_{\rm r} = (\phi_{\rm f4}(t) - \phi_{\rm f1}(t))/\Delta_{\rm r}$ and $\tilde{E}_\theta(t) = (\tilde{\phi}_{\rm f1}(t) - \tilde{\phi}_{\rm f2}(t))/\Delta_\theta$; here, $\Delta_{\rm r}$ and Δ_θ are the radial and poloidal separations of tips, respectively). In $\tilde{E}_\theta(t)$ the temperature fluctuation effect is neglected as well. The probe tips are orientated off the field lines to avoid shadowing from each other. The profiles are measured with a shot-to-shot scan, and the measurements at each radial position are carried out in several identical discharges. All the data for analysis are taken in the plasma current flat top and digitized at 1 MHz with a 12-bit resolution, using a multichannel digitizer.

To consider the poloidally sheared effect caused by $\boldsymbol{E}_{\rm r} \times \boldsymbol{B}$ rotation, an accurate measurement of the profile of the poloidal flow velocity is required. It has been reported that the $\boldsymbol{E}_{\rm r}$ phase velocity $v_{\rm p}$ of the fluctuations perpendicular to $\boldsymbol{B}$ measured with a two-point correlation technique[13,14] in the laboratory frame of reference, $v_{\rm p} = \sum_{\omega,k} \frac{\omega}{k} S(\omega,k) / \sum_{\omega,k} S(\omega,k)$, is determined by $v_E =< E_{\rm r} > /B$ effects.[15] Here, ω, k and $S(\omega,k)$ are the frequency, wavenumber and the local power spectrum density, respectively. In this paper, $< \cdots >$ represents the ensemble average over the statistically similar realizations obtained from all repeated discharge shots with 20 ms length at the same

position. Moreover, concurrent measurements on the radial profiles of E_r and the other terms of the radial force balance equation for the main ion in the ohmic confinement regime of the HT-6M tokamak have found that the E_r profile is dominated by the poloidal flow term $-v_\theta B$.[16] Therefore, in this experiment, we use the phase velocity v_p of fluctuations and v_E to estimate the poloidal flow velocity v_θ. Fig.2 shows the typical radial profiles of the poloidal phase velocity v_p, v_E and the radial electric field $< E_r >$ in the plasma boundary region. It can be seen that v_p and v_E are in close agreement. Moreover, we can find that in the proximity of the limiter radius location (r=18.2 cm), v_p, v_E and E_r change their sign. This means that a mild poloidal velocity shear layer is formed close to the last closed flux surface, in which the plasma rotates in the electron diamagnetic drift direction inside the limiter and reversely in the scrape-off layer.

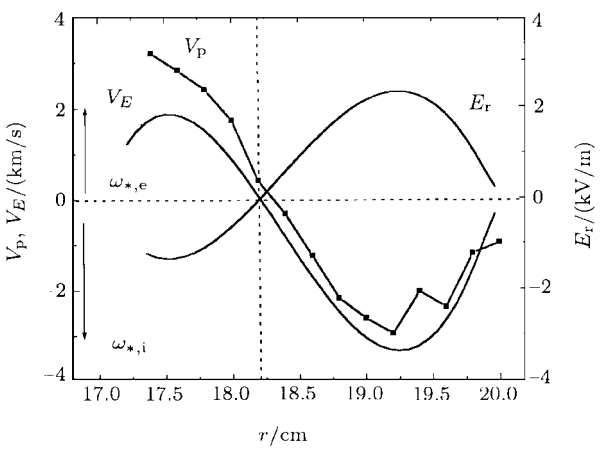


Fig.2. Radial profiles of the poloidal phase velocity v_p (line and closed squares), v_E (smooth curve) and the radial electric field E_r in the plasma boundary region. $\omega_{*,e}$ and $\omega_{*,i}$ refer to the electron diamagnetic direction and the ion diamagnetic direction, respectively.

The ACF of a time series fluctuation signal $\tilde{X}(r,t)$ is usually defined as

$$\mathrm{ACF}(r,\tau) = \frac{< \tilde{X}(r,t)\tilde{X}(r,t+\tau) >}{\sqrt{< \tilde{X}^2(r,t) >< \tilde{X}^2(r,t+\tau) >}}, \quad (1)$$

where τ is the time lag. Fig.3 shows a typical ACF curve episode of $\tilde{I}_{si}$ at the position r=18.2 cm. The curve can be divided into two sections in timescale ranges: a narrow central peak around the time lag zero and long time tails. The former carries information on the correlation of the local fluctuations (the width of the peak—the time lag corresponding to e^{-1} of the peak—stands for the turbulence decorrelation time τ_d), for the ion saturation current measured in the HT-6M tokamak, τ_d is 18 μs. The latter, corresponding to time lags much longer than τ_d but less than the confinement time (70 ms), shows a slow algebraic decay (10^{-1} ms), whose timescale is called the characteristic time of avalanches (or self-similarity). It is interesting to point out that the ACFs of the floating potential $\tilde{\phi}_f$ and turbulent transport flux have a similar characteristic property which, together with other characteristic properties (intermittent, f^{-1} noise, etc) of the edge fluctuations, forcefully display consistence with the predictions of the SOC model.

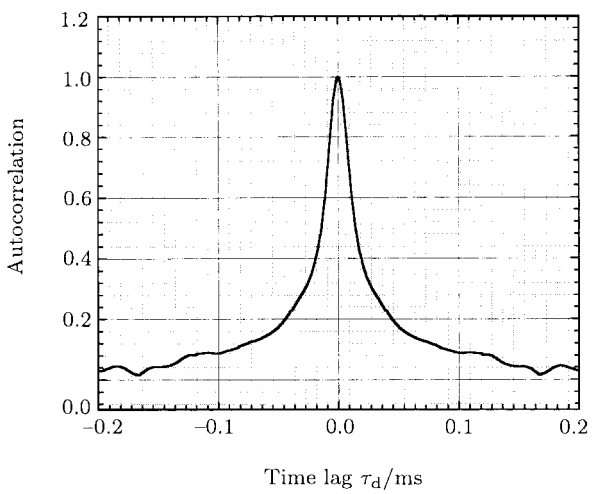


Fig.3. ACF episode of the ion saturation current measured at r=18.2 cm where E_r.

III. R/S METHOD AND DETERMINATION OF THE SELF-SIMILARITY PARAMETER

To accurately determine the slowly decaying tail of the ACF in a finite time series, a rescaled-range statistics (R/S) method based on a previous hydrological analysis by Hurst has been proposed by Mandelbrot and Wallis. This method can effectively determine the long-time correlations of the ACF in fluctuation by the Hurst exponent (H). Thus, the H exponent is called the self-similarity parameter. For a time series of length n, $Y \equiv \{Y_t : t = 1, 2, ..., n\}$, with mean value $\overline{Y}(n) = \frac{1}{n}\sum_{i=1}^{n} Y(i)$ and the standard deviation $S(n) = \sqrt{\frac{1}{n-1}\sum_{i=1}^{n}(Y(i) - \overline{Y}(n))^2}$, the R/S ratio is defined as

$$\frac{R(n)}{S(n)} = \frac{\max(0, W_1, W_2, \cdots, W_n) - \min(0, W_1, W_2, \cdots, W_n)}{S(n)}, \quad (2)$$

where $W_k = \sum_{i=1}^{k} Y(i) - k\overline{Y}(n)$. The expected value of R/S scales $E[R/S] \propto n^H$ as $n \to \infty$, where H is the Hurst exponent. For $0.5 < H < 1$, there are long-range time correlations; for $0 < H < 0.5$, the series has long-range anticorrelations; H=1 means the process is deterministic and H=0.5 corresponds to a series with short-range dependences. According to Ref.[17], in comparison with the direct determination of the ACF or other alternative techniques of H calculating, the R/S method is robust.

Methodically, we first calculate R/S in each shot data (20000 points), then average them over shots corresponding to different n to get mean R/S time series for each position, from which the H value can be obtained from the guideline of the mean R/S plot. A typical plot of R/S of $\tilde{I}_{si}$ versus the time lag τ is shown in Fig.4(a). We can see that, after the initial phase that is linked with the decorrelation time of the fluctuations τ_d, R/S tends toward an "asymptotic" power law over a broad range of time lags from an order of 10^{-1} to 10 ms. This range over which H can be determined ($H \approx 0.76$ for Fig.4(a)) is called the "self-similarity range", whose upper limit is set by the sampled data length (20 ms). The error bars are estimated by the statistical dispersion of the results from several samples of data. Fig.4(a) shows clearly that the self-similarity range is much longer than the turbulence autocorrelation time τ_d.

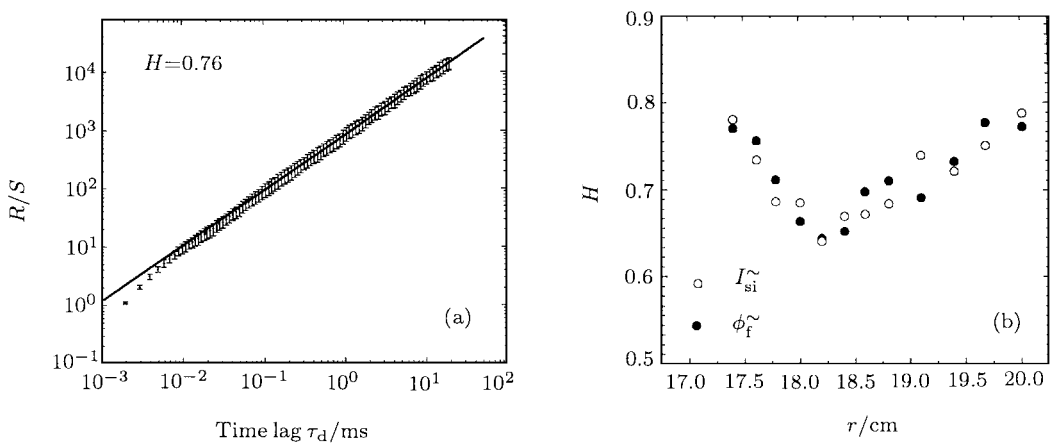


Fig.4. (a) R/S as a function of time lag for $\tilde{I}_{si}$ at r=19.6 cm. (b) Radial profiles of H values of $\tilde{I}_s$ and $\tilde{V}_f$.

According to the results of the sandpile model in Ref.[5], a sheared flow may reduce the long timescale correlation by reducing the system-scale transport events and commensurately increase the fluctuation-scale transport events to maintain a constant flux. So, experimentally measuring the radial profile of Hurst exponents versus the poloidal sheared flow is very important for identifying the edge transport mechanism of SOC model. Fig.4(b) illustrates the radial profiles of H values of $\tilde{I}_s$ and $\tilde{V}_f$. We can see that the H profiles of $\tilde{I}_s$ and $\tilde{V}_f$ are very similar with values between 0.64 and 0.79, well above 0.5. It is well worth noticing that, at the maximum velocity shear location (18.2 cm) where v_p=0, values of H of both $\tilde{I}_s$ and $\tilde{V}_f$ reach their minima ($\sim$0.64) respectively, on either side of the velocity shear layer where $v_p \neq 0$, values of H are larger. These results support the assumption of the SOC model that the shear flow may suppress long-range correlation[5] and are similar to H calculations in other devices.[6]

Of course, the long-range correlation identified here may not necessarily be long range in time. They could be caused by the long-range dependences in the poloidal variable. Because these edge flows have shear, it is not possible to resolve this ambiguity by analysing data taken at the position of zero flow. Fortunately, from the perspective of detecting signatures of SOC behaviour in plasma transport, the distinction between long range time and poloidal correlations is less important.[18] In either case, such dependences are

consistent with plasma transport mechanisms based on avalanches.

IV. PROPERTY OF THE PDF OF THE LOCAL PARTICLE FLUX

The self-similar characteristic property also exhibits itself in the PDF of the local electrostatic turbulence-induced particle flux. A local time-resolved radial particle flux is defined as $\Gamma(t) = \tilde{n}(t)\tilde{E}_\theta(t)/B$. Its normalized flux $\Gamma_{\rm n}(t) \equiv \Gamma(t)/\overline{\Gamma}$ is normalized to its time mean value. Practically, the local particle flux PDF $p(\Gamma_{\rm n})$ can be calculated by $p(\Gamma_{\rm n}) = N_{\Gamma_{\rm n}}/N$.[19] For each time sample, $N_{\Gamma_{\rm n}}$ is the number of values of $\Gamma_{\rm n}$ that fall within the range $\Gamma_{\rm n} \pm (W/2)$, where W is the length of an interval centred at $\Gamma_{\rm n}$ and N is the total number of data points in the sample. Typically, the value of $\Gamma_{\rm n}$ ranges from -20 to 20; hence, the full range of $\Gamma_{\rm n}$ values is divided into 80 intervals of equal length (W=0.5).

Figure 5 shows a typical time evolution of $\Gamma_{\rm n}$ measured in the proximity of the velocity shear layer (shot number 19509, r=18.2 cm). The flux is predominantly positive (i.e., the particle transport is outward) and intermittent. To better understand these features we integrated the transport events in terms of different amplitude and their time intervals. The results showed that nearly 50% of the total transport was carried out by those largest outward events (taken 10% of the total events, or in other words, within 10% of the time), similar results have also been obtained in other devices.[19,20] It is this property that results in a long decaying tail of the local particle flux PDF.

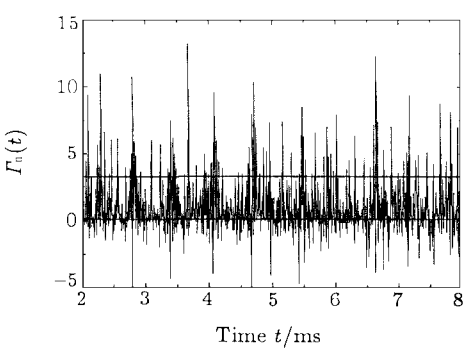


Fig.5. Time evolution episode of the local normalized particle flux $\Gamma_{\rm n}$ at r=18.2 cm where $E_{\rm r}$=0 (shot number 19509). The solid horizontal line refers to the fact that the large outward events above the line hold 50% of the total transports within 10% of the whole time.

Figure 6, the curves of $p(\Gamma_{\rm n})$ at three different radial locations, displays the asymmetrical features and long decaying tails of the flux PDF. This deviation from a Gaussian distribution is mainly caused by large amplitude transport events (bursts outwards). It is obvious in Fig.5 that the intermittence of the PDF has an order of 0.1 ms temporal repetition that is well consistent with the long correlation time of the fluctuation ACF. So, we can confidently infer that the long tail of the particle flux should be related to the self-similarity of the electrostatic turbulence-induced particle transport. In other words, this burst transport can be treated as an avalanche process characterized by the SOC model. Note that in Fig.6 the radial dependence of the local flux PDF seems slight. According to Ref.[19], the effects such as velocity shear caused by the plasma $\boldsymbol{E}_{\rm r} \times \boldsymbol{B}$ rotation and low rational q surfaces should be reflected in the symmetry of the flux PDF. Further research on this is in preparation. It also should be noted that the asymmetry of the particle flux PDF might be interpreted by other models, such as the resistive pressure-gradient-driven turbulence model, etc.[21] To distinguish them, we need to compare other features of the local turbulence-induced particle transport flux. The most relevant distinction between models is in the different characteristic radial scale length of the flux.[19] So, it is our present study to compare the correlations of fluxes at different radial positions.

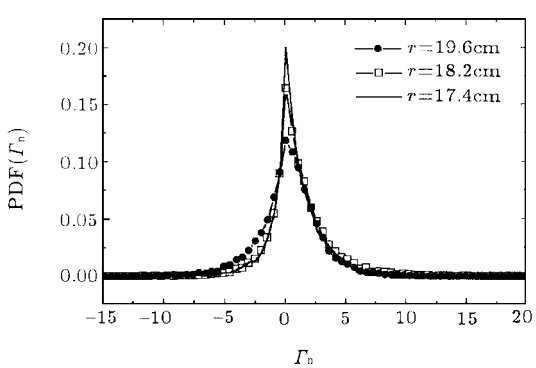


Fig.6. Comparison of the flux PDFs of three positions in the velocity shear layer.

V. CONCLUSIONS

To better understand long timescale transport dynamics, we apply the R/S analysis, the ACF and the PDF statistical analyses to investigate the long time range dependences of edge plasma fluctuations in an HT-6M tokamak. The results display the self-similar characters of the electrostatic fluctuations with self-similarity parameters (Hurst exponent) ranging from 0.64 to 0.79, taking into consideration the $\boldsymbol{E}_{\rm r} \times \boldsymbol{B}$ rotation sheared effect. Both ACFs of $\tilde{\phi}_{\rm f}$ and $\tilde{I}_{\rm si}$ and PDF of the turbulence-induced particle flux have two

distinct timescales. One corresponds to the decorrelation timescale (of the order of μs) of local fluctuations and the other lasts much longer than the former and less than the confinement time (of the order of ms). The asymmetric profile of the PDF reveals the outward bursting property of the local particle flux. Despite the fact that there might be other interpretations for it, the characteristic feature of the flux PDF is in close agreement with the predictions of the SOC model. All these experimental results suggest that some of the mechanisms of the underlying turbulence are consistent with the plasma transport as characterized by SOC.

ACKNOWLEDGMENTS

The authors gratefully acknowledge the support of the HT-6M group for the operation of the tokamak. Thanks are due to Professor J. R. Luo for helpful discussions, and it is a pleasure to thank Dr. Baoyi and Ms. A. L. Yao for technical assistance.

References

[1] Liewer P C 1985 *Nucl. Fusion* **25** 543
[2] Wootton A J *et al.* 1990 *Phys. Fluids* B **2** 2879
[3] Perkings F W *et al.* 1993 *Phys. Fluids* B **5** 477
[4] Diamond P H and Hahm T S 1995 *Phys. Plasmas* **2** 3640
[5] Newman D N, Carreras B A, Diamond P H and Hahm T S 1996 *Phys. Plasmas* **3** 1858
[6] Carreras B A *et al.* 1998 *Phys. Rev. Lett.* **80** 4438
[7] Van Milligen B Ph *et al.* 1998 Proceedings of 17th IAEA Fusion Energy Conference
[8] Pedrosa M A *et al.* 1999 *Phys. Rev. Lett.* **82** 3621
[9] Carreras B A *et al.* 1999 *Phys. Plasmas* **6** 1885
[10] Mandelbrot B B and Wallis J R 1969 *Water Resour. Res.* **4** 909
[11] Hurst H E 1951 *Trans. Am. Soc. Civil Eng.* **116** 770
[12] Lin H *et al.* 1992 *Rev. Sci. Instrum.* **63** 4611
[13] Beall J M *et al.* 1982 *J. Appl. Phys.* **53** 3933
[14] Levinson S J *et al.* 1984 *Nucl. Fusion* **24** 527
[15] Tsui H Y *et al.* 1993 *Phys. Fluids* B **5** 2491
[16] Xu Y, Yu C X *et al.* 1998 *Phys. Plasmas* **5** 2317
[17] Mandelbrot B B and Wallis J R 1969 *Water Resour. Res.* **5** 967
[18] Carreras B A *et al.* 1998 *Phys. Plasmas* **5** 3632
[19] Carreras B A *et al.* 1996 *Phys. Plasmas* **3** 2664
[20] Endler M *et al.* 1995 *Nucl. Fusion* **35** 1307
[21] Carreras B A, Garcia L and Diamond P H 1987 *Phys. Fluids* **30** 1388